J. Fluid Mech. (1970), *vol.* 41, *part* 4, *pp.* 707–719
Printed in Great Britain

Observations of the cell structure of salt fingers

By T. G. L. SHIRTCLIFFE† AND J. S. TURNER
Department of Applied Mathematics and Theoretical Physics,
Cambridge University

(Received 10 October 1969)

The phenomenon of salt fingers has been investigated optically to determine the geometry of the cells as seen from above. When the fingers are short, the flow appears to be highly turbulent, though a dominant scale is evident. When the fingers are longer, a cellular structure is clear. This structure changes only slowly, apparently in response to disturbances in the convecting layers which bound the fingers above and below, and becomes more nearly stationary as the fingers grow. Cell boundaries show a strong tendency to intersect at right angles, which favours the emergence of cells with a square horizontal section. As the fingers get longer the cell width increases, but more slowly than the length.

1. Introduction

The phenomenon of salt fingers was first described by Stern (1960). He derived the criterion for marginal stability and went on to show that, although at marginal stability the flow occurs with a cell width comparable to its depth, under supercritical conditions the fastest-growing cell is much narrower. A more formal analysis of conditions near marginal stability has recently been given by Baines & Gill (1969) for the whole class of instabilities which occur when a fluid contains vertical gradients of two diffusing components.

These analyses make the usual assumption that there is a linear variation in concentration of each diffusing component between bottom and top of the container. In practice, salt fingers are more easily studied when they occur at an interface between two homogeneous layers of liquid. This arrangement was used by Turner (1967) in an experimental study of the rates of transport of the two components, salt and heat, by the fingers. Turner's paper contains a photograph which gives a good indication of the columnar nature of the fingers.

The principal interest in salt fingers lies in the very high rates of vertical transport of salt and heat which they could potentially produce in the ocean, in the case of warm saline water overlying cold fresher water. However, although the diffusivity of heat in water is about 100 times greater than that for salt, the phenomenon occurs also when the diffusing components have diffusivities which are much more nearly equal. It is only necessary that the faster-diffusing component should be stabilizing, that the slower-diffusing component should be destabilizing, and that the combined density effects should appear gravitationally stable without, however, exceeding the condition for marginal stability. Stern & Turner

† On leave from the Victoria University of Wellington, New Zealand.

(1969) therefore used salt and sugar as the two diffusing components; this avoided the difficulties associated with heat losses by conduction through the tank walls and also allowed a much greater range of concentrations to be studied. Since salt diffuses in water more rapidly than sugar, the fingers were produced at the interface between a more dense salt solution and an overlying, less dense sugar solution.

The experiments reported by Stern & Turner consisted of measurements of bulk properties of the system, such as growth rates of the fingers and rates of transport of the solutes, together with qualitative observations of the behaviour when the variation of solute concentration with height is linear. These experiments were supported by dimensional arguments and order-of-magnitude calculations. Similar calculations have been performed by Stern (1969) concerning the more detailed question of the interaction between members of a group of fingers. However, it appears that a thorough understanding of the phenomenon must await the availability of detailed observations of the structure of the fingers. This paper reports an attempt to establish the planform of salt finger cells, produced in water with sugar and salt as the solutes.

2. The nature of the system

The experiments were carried out in a Perspex tank which was 12·5 cm deep, and 15 cm by 5 cm horizontally, all measurements being internal ones. Initially, the tank was half filled with a homogeneous, air-free solution of common salt in water. A similar solution of sugar, rather less dense than the salt solution, was poured carefully onto the salt until the tank was full. A Perspex lid was then screwed on, air bubbles being carefully avoided, so that there was no meniscus at the top of the tank. The tank was placed in the vertical collimated light beam of a schlieren system, and avoidance of a liquid meniscus allowed observations to be made right up to the tank wall.

Observations made with a vertical light beam can only be interpreted if something is known of the nature of the regions through which it passes. Figure 1, plate 1, is a typical shadowgraph produced by shining a collimated light beam horizontally through the tank and onto a screen. (The tank used in this example differs from that used in the present experiments in having no lid.) It is clear that there are three main regions, namely the top and bottom convecting layers, and the fingers between them. The convection is associated mainly with plumes or sheets of material ejected from the finger region, and these wander laterally in a haphazard manner. Only the finger region shows any regularity of structure. The fingers are apparently disturbed by the convection only close to their ends, where there is some lateral motion produced by the irregular shear flow.

3. The method of observation

The optical system is sketched in figure 2. The light source was a 1 mW helium–neon laser whose beam was expanded to a diameter of 5 cm. Since it was convenient to use a horizontal optical bench, four front-surface plane mirrors deflected the horizontal beam to the vertical, and brought it back to its original

axis after passing through the tank. The beam was then focused by a lens onto an aperture whose diameter was adjustable. The same lens produced an image of the tank as seen from above; points nearer the top of the tank were brought to an image further beyond the focal plane. An eyepiece lens was placed beyond the focal plane to inspect this image. Because of the aperture, only light which had suffered very little deflexion was transmitted to the image. Thus the image showed those areas in the tank where the angular deflexion of the light was less than a limit determined by the ratio of the aperture radius to the focal length of the lens (15 cm). Most observations were made with an aperture of radius 0·15 cm, allowing a maximum deflexion of 0·01 radian, although radii down to 0·025 cm were available.

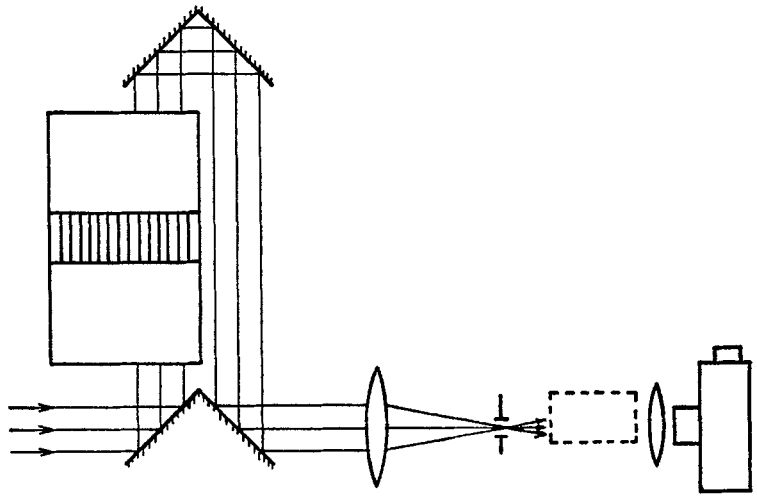

FIGURE 2. The optical system used to observe the cell structure of the fingers.

Since the maximum deflexion produced in the system seldom exceeded 0·04 radian, it may seem that the acceptance of deflexions up to 0·01 radian was rather unselective. There were two reasons for choosing this value. First, if only very small deflexions were accepted by the system, the image was made up of an array of bright dots, each of which corresponded to a point of zero deflexion, that is, zero horizontal gradient of refractive index. While this gave an idea of the regularity of the refractive index field (figure 13(*c*)), it gave no direct information on the shape of the cells. By accepting greater deflexions, it became possible to see a more complete outline of the cells.

The second reason for using a relatively large aperture was that it allowed a distinction to be made between those illuminated regions which contained maxima and those which contained minima of refractive index. The deflexions produced by these two cases appeared to arise in or near two planes which lay respectively above and below the mid-plane of the fingers. Thus by moving the eyepiece lens along the optical bench, either one of these planes could be brought into focus. With a small aperture, the depth-of-focus was large and the two planes were indistinguishable. With a large aperture, however, the depth-of-focus was

reduced and the image could be clearly resolved into two complementary patterns, either of which could be brought into quite sharp focus while the other remained poorly defined. On all illuminated points of one pattern, the refractive index was a near-maximum, while on the other it was a near-minimum.

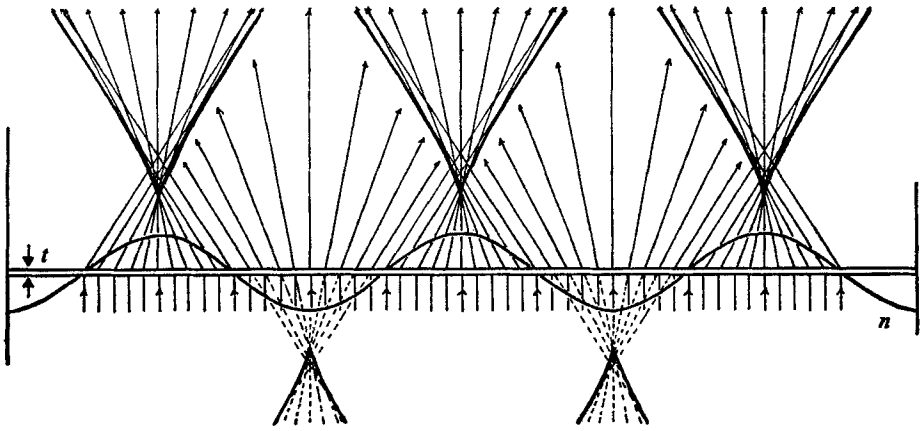

FIGURE 3. The focusing effect of a thin layer containing a sinusoidal distribution of refractive index. The cusped curves are the caustics, or loci of the focal points for various positions along the layer. Most of the light passes (or appears to pass) very close to the cusps, which are the 'ideal' focal points.

The origin of these two planes from which the deflexions appeared to arise may be seen most easily in relation to a one-dimensional sinusoidal variation of refractive index in a thin horizontal layer, through which a vertical collimated beam of light passes; the extension to a further dimension is straightforward. Let the refractive index in the layer be

$$n = n_0 + n_1 \sin kx,$$

the material above and below the layer having refractive index n_0. Then if t is the thickness of the layer, rays which are perpendicular to it at incidence are deflected through an angle θ, where

$$\theta = (t/n_0)\, dn/dx = (tkn_1/n_0) \cos kx.$$

Taking z in the direction of propagation before the light strikes the layer, with origin in the layer, we may calculate the point $(x+\Delta x, \Delta z)$ through which pass all the rays which traverse the layer between x and $x+dx$; this is the centre of curvature of that part of the emergent wave front which lies between x and $x+dx$, or the focal point for light in that interval. It is easy to show that, for small θ,

$$\Delta x = (k \tan kx)^{-1},$$

$$\Delta z = n_0/(tk^2 n_1 \sin kx).$$

The locus of $(x+\Delta x, \Delta z)$, that is the caustic of the system, is the cusped curves in figure 3; typical rays are also plotted on this diagram. It is clear that there is a marked focus above each maximum of n and below each minimum, the latter

being a virtual focus. Those rays which are not greatly deflected produce sharp focuses a distance $n_0/(tk^2n_1)$ above and below the layer. Only the rays with nearly the maximum deflexion fail to pass very close to this focus. To be more specific, 50 % of the light passes closer than $0{\cdot}04\lambda$ to the 'ideal' focus ($\lambda = 2\pi/k$) and this includes all the light which is deflected through angles less than 70 % of the maximum.

It has been assumed here that the layer in which the deflexions are produced is a thin one, and that the refractive index varies only in the horizontal. The question of what constitutes a thin layer in this context has been considered by Shirtcliffe (1969); the approximation is justified provided that

$$(\tfrac{1}{6}t^2)\{2(dn/dx)^2/n_0^2 + (d^2n/dx^2)/n_0\} \ll 1.$$

In all the observations to be discussed in this paper, this condition is fulfilled. With regard to the second assumption, if refractive index varies also in the vertical, the vertical component of the refractive index gradient does not contribute to the deflexion. θ is therefore determined by the mean value of the horizontal gradient, averaged along the ray path through the layer.

4. The observations

Six runs were made to cover a range of values of the initial concentrations of the sugar and salt solutions. The behaviour was qualitatively the same in each run. The interface was very turbulent initially; there was no regular pattern visible, and all deflexions of the light beam originated close to the plane of the interface. As a result of the transport of sugar and salt across the interface, the difference in concentration of each of these across the interface decreased with time; the motions became slower, the fingers became longer, and a dominant scale appeared. In due course the dominant scale developed into an increasingly steady pattern, the scale of which slowly increased. The optical patterns were sharply defined in two planes which were both indistinguishably close to the mid-plane of the fingers initially, but which slowly moved apart symmetrically above and below that plane; these planes could only be located within about $\pm$ 1 cm. Linear disturbances were seen to cross the field of view from time to time, and it is likely that these were associated with the convection adjoining the fingers; if so, the convection proceeds by way of two-dimensional sheets rather than plumes from point sources, but the optical effect was not large.

As the cellular pattern developed, the sides of the cells showed a strong tendency to meet at right angles, and it seems clear that the preferred planform for the flow is one having square cells. The tank has a marked effect; the pattern was oriented so that the sides of the squares were parallel and perpendicular to the wall for several cell widths from the wall. However, the sides which were perpendicular to the wall showed a weaker tendency to be aligned than those which were parallel to it. At the most, seven cells were seen to be aligned (within $\pm\frac{1}{4}$ cell width) perpendicular to the wall, and it was uncommon to see more than three.

The photographs in figures 4 to 11, plates 2 and 3, show a sequence from one

run, during which the finger length increased from 0·25 to 3·5 cm. The first five photographs show both patterns in focus at the mid-plane of the system. Thereafter the separation of the planes in which the patterns were focused warranted separate photographs. Note that on each photograph both patterns appear, only one being sharply defined.

Figures 12(*a*) and (*b*), plate 4, are taken from another run when the fingers were 4·5 cm long, and show more clearly the complementary patterns. These photographs were taken in the corner of the tank to see if any special effects occurred there. Some tendency for the cell boundaries to curve round the corner is apparent, but this seems more likely to be an effect of the larger scale motion in the convecting layers than to be due to the tank walls acting directly on the fingers.

Figures 13(*a*), (*b*) and (*c*), plate 4, are included to show the effect of reducing the size of the schlieren aperture. These photographs were taken during the same run as those in figure 12, at an earlier stage when the fingers were 3·5 cm long. In figure 13(*c*) the aperture is 0·075 cm in radius, half that used in all the other photographs presented here. It is difficult to compare these three photographs point by point, but it is clear that most of the features of figures 13(*a*) and (*b*), whether lines or dots, in focus or out of focus, appear in figure 13(*c*) as fairly well-defined dots or crosses. Equally clearly, photographs using the wider aperture give a clearer picture of the cellular structure than does the one using a small aperture. However, by making observations visually rather than photographically, focusing on the patterns in turn, and using a range of aperture sizes, it is possible to build up a qualitative picture of the distribution of refractive index which exists in the fingers.

For example, it is found that the small crosses in figure 13(*c*), for which photograph the camera was focused on the mid-plane of the fingers, resolve themselves into one of their component lines in the upper focal plane, and the other component line in the lower focal plane. The former line shows the axis of a maximum of refractive index, the latter the axis of a minimum; the point where these cross is therefore a saddle-point.

5. The dominant patterns

In all runs of the experiment, as the cells became less disturbed, one particular structure became dominant in them; examples of this appear throughout figures 9–13. The structure is sketched in figures 14(*a*) and (*b*), as seen in the two focal planes respectively above and below the mid-plane of the fingers. It is made up of dots indicating maxima of refractive index (focused in figure 14(*a*)) and minima (focused in figure 14(*b*)), and lines indicating saddle-points. Putting these together, it is clear that the distribution of refractive index which gives rise to this structure is qualitatively similar to that shown in figure 15, which shows the contours of a $\sin kx \sin ky$ surface drawn with its scale and orientation corresponding to those of figure 14. The refractive index therefore has a distribution of approximately this form, although the extent to which it departs from it in detail is not known.

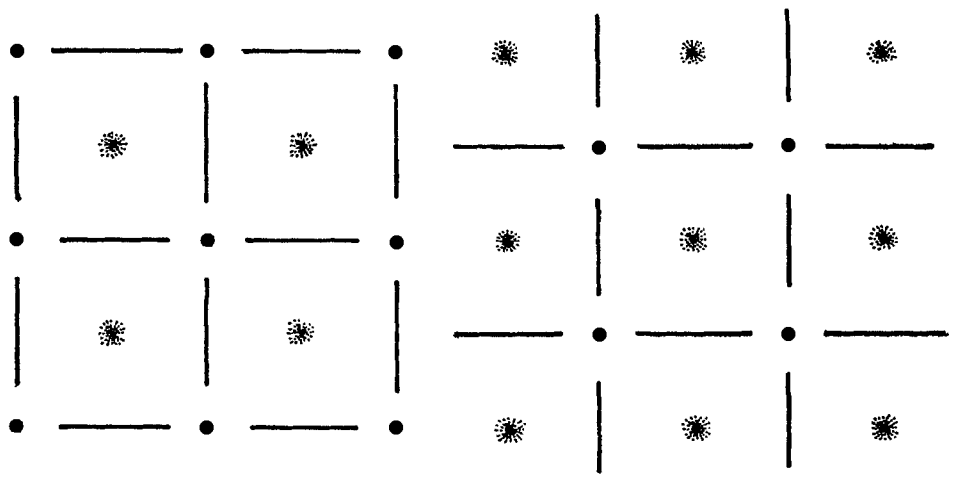

(*a*) (*b*)

FIGURE 14. Sketches of the dominant pattern: (*a*) as seen in the upper focal plane, and (*b*) the corresponding form in the lower focal plane.

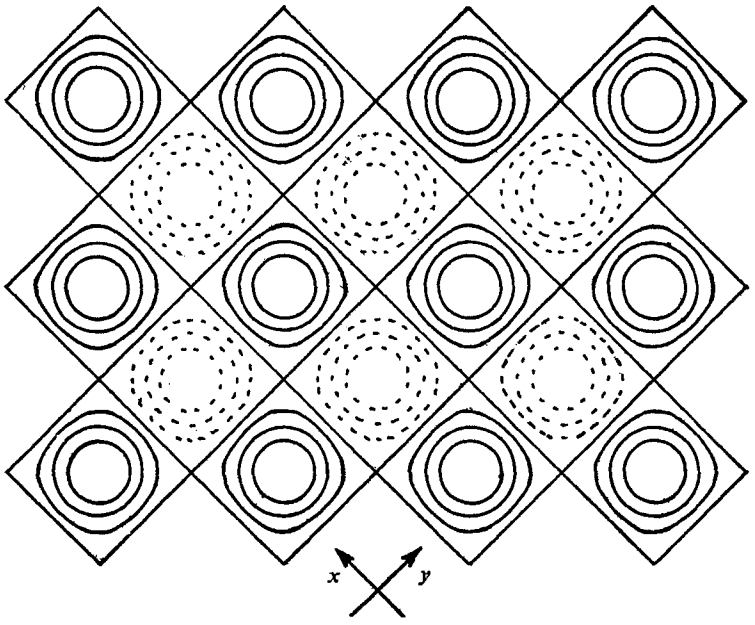

FIGURE 15. The contours of a $\sin kx \sin ky$ surface. A refractive index distribution of similar form would yield the pattern drawn in figure 14.

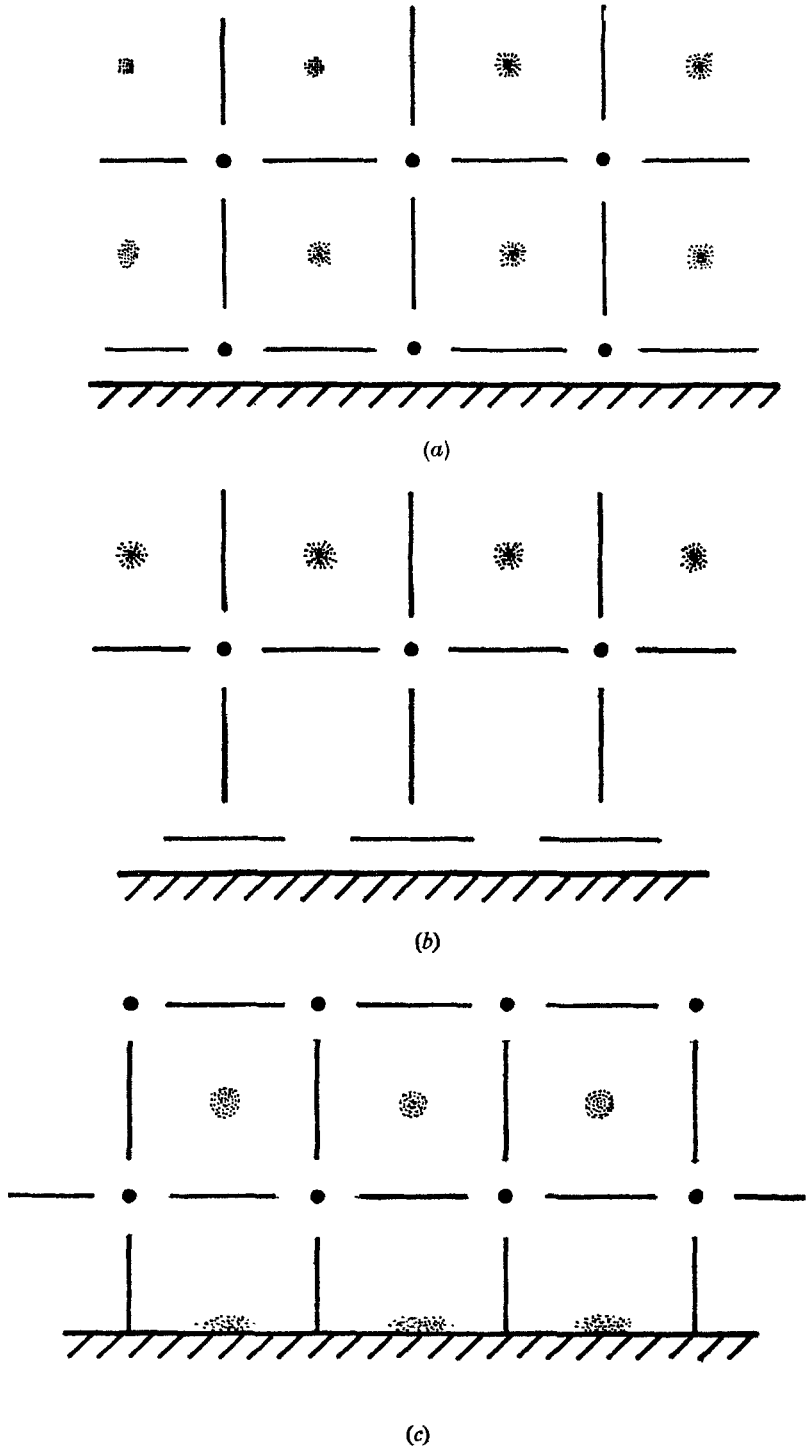

FIGURE 16. (*a*) and (*b*) Two forms of the pattern seen most often near the walls of the tank, in the upper focal plane. (*c*) The form of the pattern in the lower focal plane, corresponding to both (*a*) and (*b*).

Near the tank wall the pattern tended to be similar to that which dominated the interior of the tank. An invariable feature was that the squares in the observed pattern aligned themselves so that their sides were perpendicular and parallel to the wall. An unexpected feature was that in almost every case the part of the pattern nearest the wall consisted of lines parallel to the wall (with or without dots between them) in the upper focal plane, and lines perpendicular to the wall in the lower focal plane. This situation is idealized in the sketches of figure 16; (*a*) and (*b*) show alternative forms of the pattern in the upper focal plane, while (*c*) is the pattern corresponding to either of these in the lower plane. As the photographs show, the pattern was rather variable near the wall, and figure 16 is included here only because it is probably the best estimate that can be made of a typical pattern. It was unexpected because it implies that maxima of refractive index lay along the wall in almost every observation, whereas *a priori* maxima and minima seem equally probable.

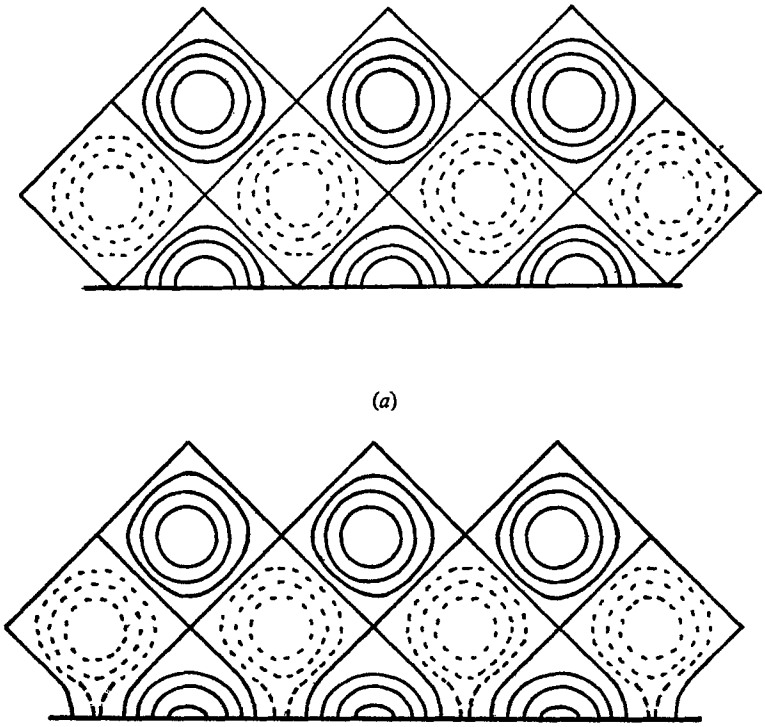

FIGURE 17. (*a*) Contours of the refractive index distribution corresponding to figure 16(*a*) and (*c*). (*b*) The distribution corresponding to figures 16(*b*) and (*c*).

Figure 17(*a*) shows the refractive index distribution corresponding to the patterns of figures 16(*a*) and (*c*), while figure 17(*b*) corresponds to figures 16(*b*) and (*c*). Figures 17(*a*) and (*b*) are very similar, and are both reasonable in the sense that they satisfy the condition that the gradient of concentration of salt and

sugar, and hence the gradient of refractive index, perpendicular to the wall should be zero at the boundary.

The lines which run perpendicular to the wall in figure 16 were sometimes less bright than those parallel to the wall, showing that they intercepted a smaller area of the incident light beam. Occasionally they were absent, in which case the 'fingers' consisted locally of sheets parallel to the wall, rather than columns.

A final point which deserves mention concerning the observed patterns is that they were more easily discerned in the upper focal plane than in the lower, as may be seen in figures 9–13. This is because the part of the pattern which was in focus in the upper focal plane and out of focus in the lower plane was brighter than the other part. The effect seems to be real rather than instrumental, and implies that a greater proportion of the incident light beam was concentrated into the upper focused pattern by the maxima of refractive index than was concentrated into the lower focused pattern by the minima. The possibility therefore exists that there is an asymmetry between the regions of high and those of low refractive index. It is not clear how this can be reconciled with the (approximate) observation that the focal planes were disposed symmetrically above and below the mid-plane of the fingers; a more sophisticated experiment is needed to establish the refractive index distribution in detail.

6. The flow patterns

Up to this point, the discussion has been concerned with optics; certain cellular images have been demonstrated, and the corresponding distributions of refractive index deduced. Primary interest attaches, however, to an understanding of the distributions of such quantities as density, salt concentration, sugar concentration and velocity.

Figure 18 shows the dependence of refractive index and of density on the concentration of sugar and salt in aqueous solution. The refractive index contours were derived from 21 measurements with an Abbé refractometer, evenly spaced over the field, to which a second-degree function was fitted. It may be seen that refractive index is not uniquely determined by the density of the solution, although the contours of both are nearly parallel. In principle, it is possible that a denser, more salty solution may have a lower refractive index than a less dense solution containing more sugar. However, this is not thought to apply in any of the observations, and the distributions of refractive index shown in figures 15 and 17 can probably be interpreted qualitatively by reading 'density' for 'refractive index'. In either case, of course, what is plotted is the horizontal distribution of a mean taken along a vertical path through the fingers, since the light beam samples all levels. It is thought that the density (and refractive index) increases with depth along any vertical, but it remains true that the velocity is directed downwards where the 'density' in figures 15 and 17 is a maximum, and upwards where it is a minimum.

Assuming symmetry between upward and downward flow, since the velocity is extremal where the density is too, the velocity is zero along the lines $\sin kx = 0$ and $\sin ky = 0$ in figure 15. The smallest unit of the flow pattern which it is

reasonable to call a cell is a square of side $(2\pi/k)$, which includes four individual fingers, two flowing upwards and two downward. This 'cell' must be distinguished from the square which appears as a unit of the optical pattern in figure 14, from which figure 15 is derived. The latter is formed in figure 14(*a*) by joining adjacent points of maximum downward velocity, and in figure 14(*b*) by joining adjacent points of maximum upward velocity; it has a side of length $(\sqrt{2}\pi/k)$, and is oriented at 45° to the flow cell.

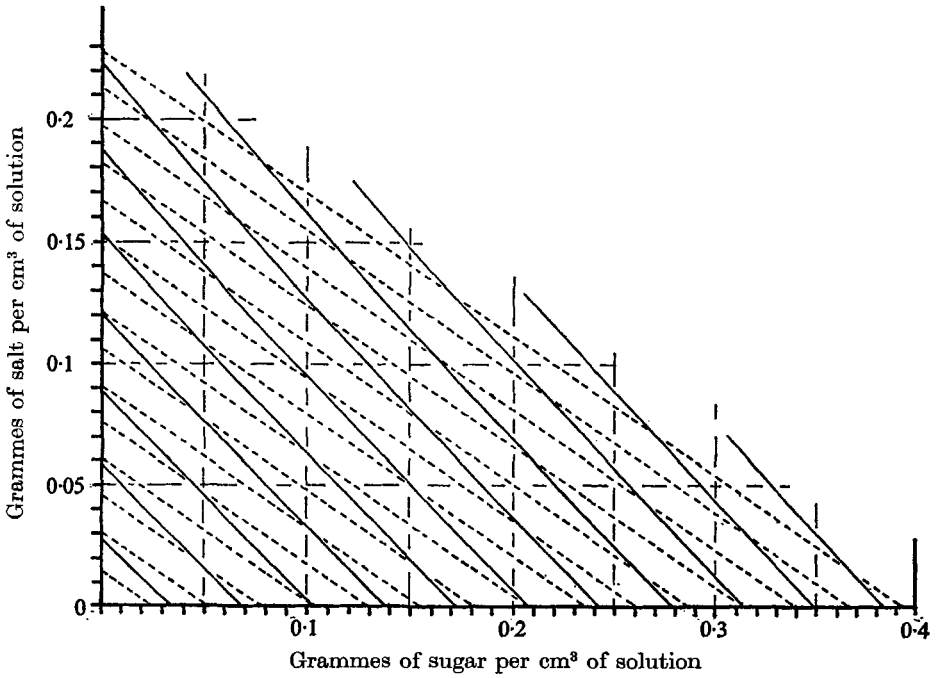

FIGURE 18. The dependence of refractive index and density on the concentration of salt and sugar in aqueous solution. The contours of refractive index (———) are shown at increments of 0·005, and those of density (- - - - - - -) at increments of 0·01 g cm^{-3}, with respect to pure water.

A similar argument applies to figure 17. Here the velocity is downward in all the fingers located along the wall, and zero along the straight contours inclined at 45° to it. The velocity must, of course, be zero also just at the wall. Note that a pattern in which the zero velocity contours are parallel and perpendicular to the wall, with upward and downward velocities alternating, could also satisfy the diffusion boundary conditions, although of course there must again be local distortions near the wall. The corresponding optical cells with boundaries at 45° to the wall have, however, never been observed, for reasons which we do not properly understand.

7. The growth of the cells

It may be seen from figures 4 to 11 that the width of the cells increased as their length, that is the length of the fingers, increased; figure 19 shows this behaviour in more detail. The measurements of width were made by placing a scale in front

of the eyepiece lens, coincident with the image of the tank. The measurements of optical cell width have been multiplied by $\sqrt{2}$ to convert them to wavelength (λ) in the corresponding flow pattern.

When the fingers were very short, the flow was rapid and confused, and the values of width which were adopted were subjective assessments of the dominant scale. At the worst, this assessment might have been in error by a factor 2 either way. As the fingers grew, it became easier to define a scale for them, and the uncertainty in cell width decreased. A comparison of figures 6 and 7 shows that the cell boundaries became reasonably clear when the length approached 1 cm.

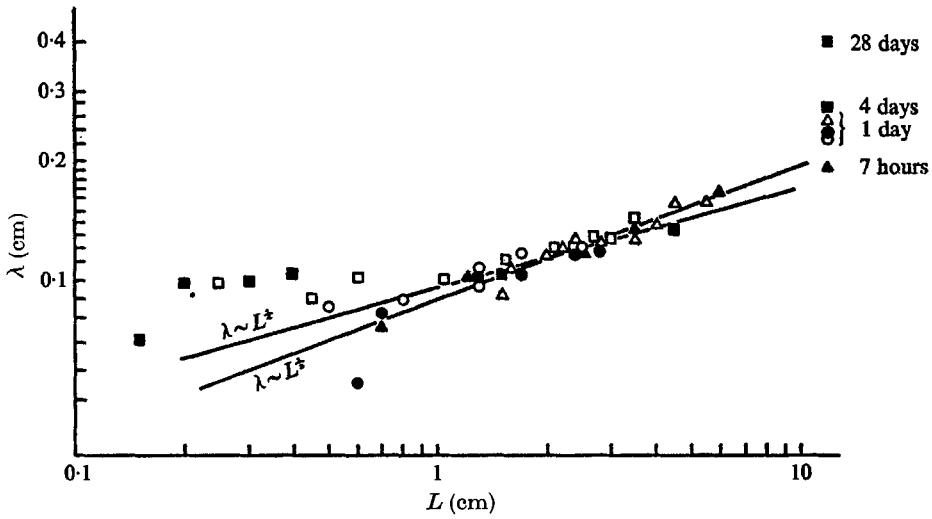

FIGURE 19. The wavelength of the cells in planform, as a function of finger length. The points are from run 1 (○) (densities of initial sugar and salt solutions 1·09 and 1·10 g cm^{-3}; run 2 (△) (1·09/1·10); run 3 (□) (1·10/1·11); run 4 (●) (1·05/1·06); run 5 (▲) (1·045/1·05); run 6 (■) (1·11/1·12). The points plotted at 12 cm are for fingers which extended throughout the depth of the tank; the time given against each point is that since the tank was filled.

The values beyond a length of about 4 cm are perhaps suspect, since the tank was only 12 cm deep, and some 'end effect' might have occurred. One observation which should be mentioned here is that 'secondary fingers' sometimes formed at the top and bottom of the tank. These were very weak, and were generally of different length and width to the fingers being studied, so they should not have affected the optics significantly. They appeared to form at the beginning of a run, as a result of the convective sheets in the mixed layers. These apparently produced a mild stratification near the top and bottom of the tank which favoured the onset of fingers; these secondary fingers grew rapidly to a length of about 2 cm and then stabilized. Their optical effect on a horizontal beam of light was much less than that of the primary fingers, even when the latter were longer than 2 cm, and the effect is not thought to have interfered with these observations to any significant degree.

The graph of figure 19 may be accepted without reservation, then, only for lengths between about 1 and 4 cm. However, this section is sufficient to show

that the width does not increase in proportion to the length as might be expected from the simplest similarity argument, which gives a single length scale if the dependence on the concentration differences between the two convecting layers is neglected (Stern & Turner 1969, § 2.1). In fact the width increases as the one-third or one-quarter power of the length in this range.

When the fingers had grown to occupy the whole depth of the tank, they did not disappear. The cell width increased very slowly, and the refractive index gradients decreased, but the effects were still observable many days later. Several readings from this régime are included in figure 19, plotted at a length of 12 cm. The point from run 5 was obtained 7 h after the tank was filled, when the fingers had just grown to 12 cm. The groups of points from runs 1, 2 and 4 were obtained between 19 and 23 h after the tank was filled. The lower point for run 6 represents 4 days, and the upper point 28 days, after filling. It is clear that the point from run 5 lies near the extrapolated line of the runs for short fingers, so it seems possible that there was in fact no change in the mechanism which governed the cell width from the time when a clear cellular pattern was first established at a length of about 1 cm until the fingers extended throughout the container.

The first author is grateful for support given at different times during this work through a Royal Society and Nuffield Foundation Commonwealth Bursary, and a New Zealand Post-Doctoral Fellowship. The second author, and the experimental work in Cambridge, were supported by a grant from the British Admiralty.

REFERENCES

BAINES, P. G. & GILL, A. E. 1969 On thermohaline convection with linear gradients. *J. Fluid Mech.* **37**, 289.

SHIRTCLIFFE, T. G. L. 1969 A dual-purpose schlieren system. *J. Sci. Instrum.* **2**, 963.

STERN, M. E. 1960 The 'salt-fountain' and thermohaline convection. *Tellus*, **12**, 172.

STERN, M. E. 1969 Collective instability of salt fingers. *J. Fluid Mech.* **35**, 209.

STERN, M. E. & TURNER, J. S. 1969 Salt fingers and convecting layers. *Deep-Sea Res.* **16**, 497.

TURNER, J. S. 1967 Salt fingers across a density interface. *Deep-Sea Res.* **14**, 599.

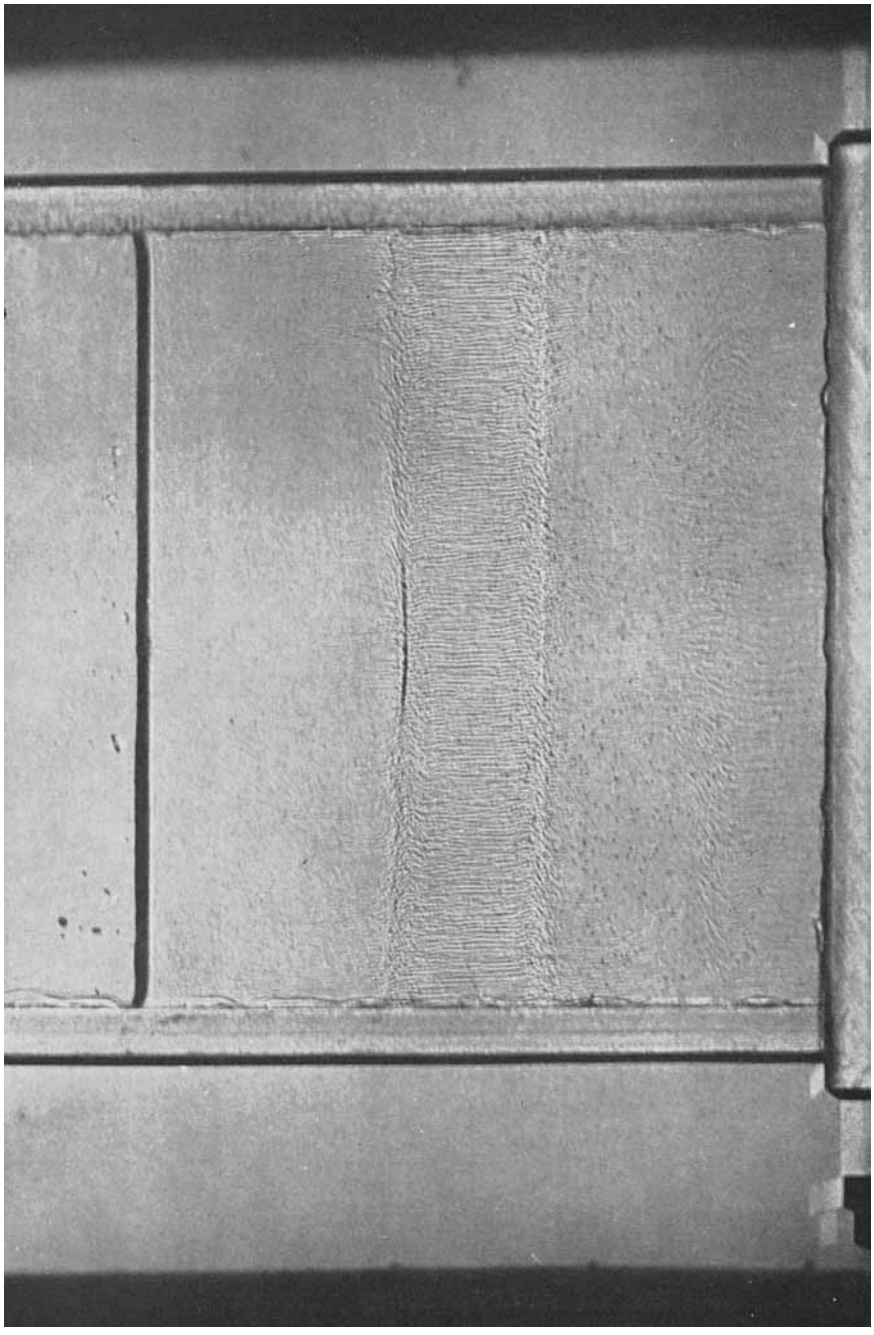

FIGURE 1. A shadowgraph produced by shining a horizontal collimated beam of light through the tank and onto a screen. The salt fingers occupy the central layer, with convecting regions above and below.

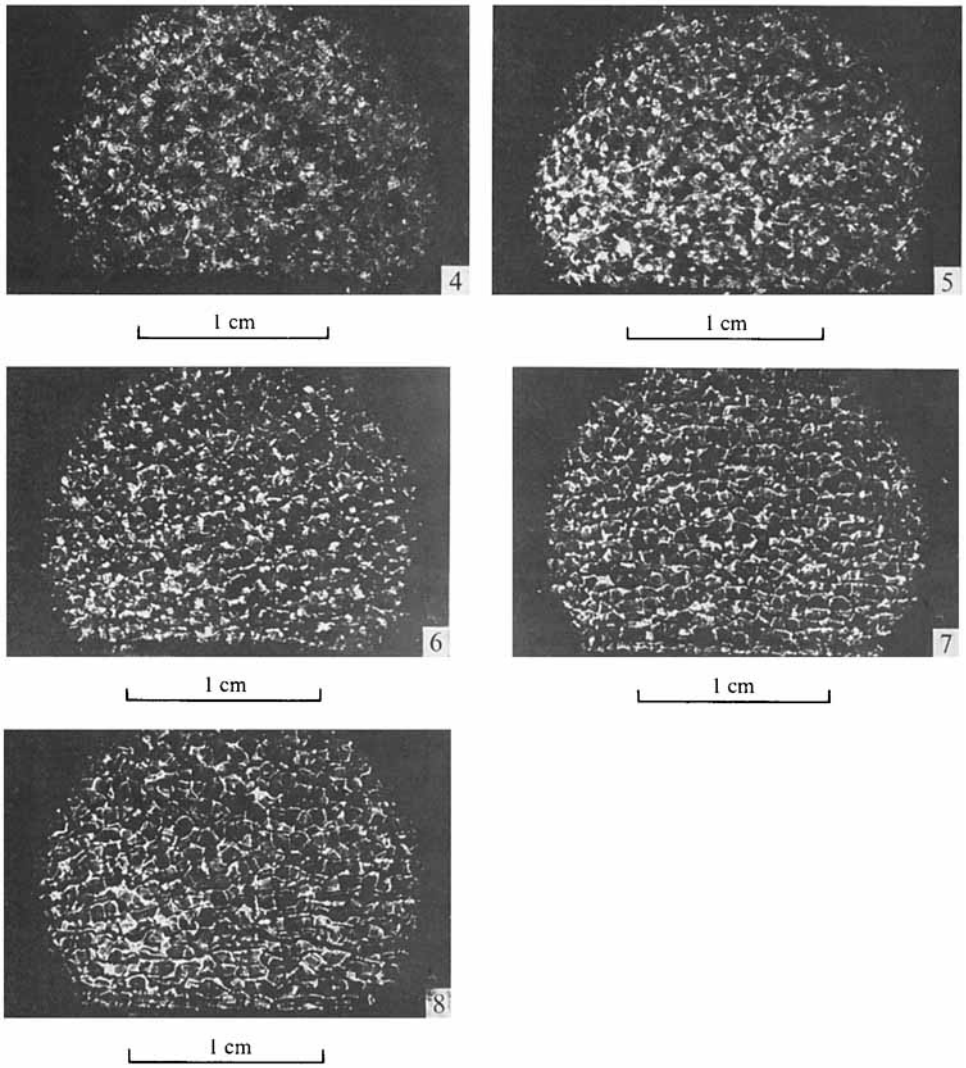

FIGURE 4. The first of a sequence of photographs showing the development of the cell planform in a typical run (run 3). This photograph was taken 30 min after the tank was filled, when the fingers were 0·25 cm long. In figures 4–8 the camera was focused on the mid-plane of the fingers. The tank wall is at the bottom of each photograph.

FIGURE 5. Total time 60 min, fingers 0·45 cm long.

FIGURE 6. Total time 85 min, fingers 0·6 cm long.

FIGURE 7. Total time 115 min, fingers 1·05 cm long.

FIGURE 8. Total time 148 min, fingers 1·55 cm long.

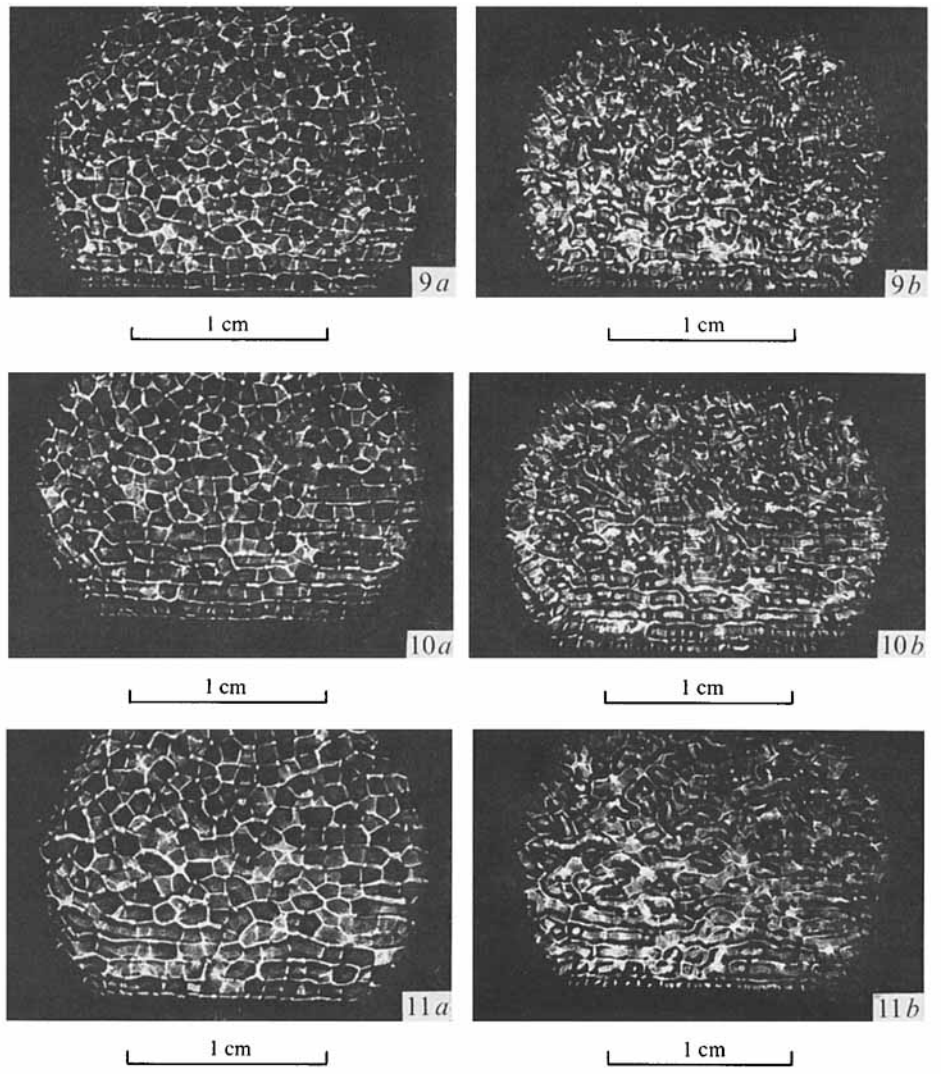

FIGURE 9. A continuation of the sequence from run 3. Total time 180 min, fingers 2·1 cm long. (*a*) The pattern seen in the upper focal plane. (*b*) The pattern seen in the lower focal plane.

FIGURE 10. Total time 222 min, fingers 2·7 cm long. (*a*) and (*b*) as in figure 9.

FIGURE 11. Total time 260 min, fingers 3 cm long. (*a*) and (*b*) as in figure 9.

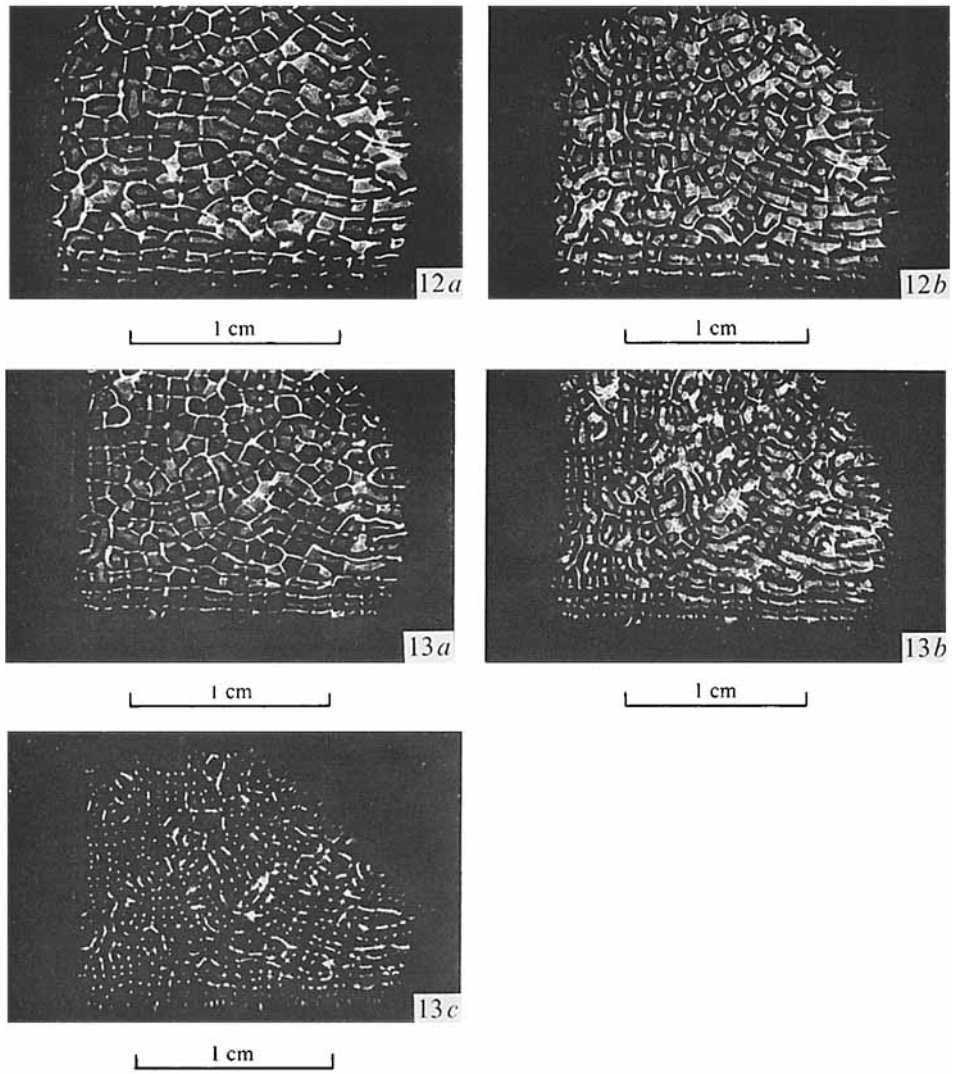

FIGURE 12. Photographs from run 2 of the patterns near the corner of the tank. Total time 342 min, fingers 4·5 cm long. (*a*) and (*b*) as in figure 9.

FIGURE 13. Photographs from run 2 showing the effect of reducing the radius of the schlieren aperture. Total time 266 min, fingers 3·5 cm long. (*a*) and (*b*) as in figure 9. (*c*) The pattern seen in the mid-plane of the fingers when the aperture radius was 0·075 cm, compared with 0·15 cm for all the other photographs.